RECEIVED BY TIC JUN 2 8 1972

ISOTOPIC POWER MATERIALS
DEVELOPMENT PROGRESS REPORT
FOR MAY 1972

R. G. Donnelly

OAK RIDGE NATIONAL LABORATORY
OPERATED BY UNION CARBIDE CORPORATION • FOR THE U.S. ATOMIC ENERGY COMMISSION

DISCLAIMER

DISCLAIMER

Portions of this document may be illegible in electronic image products. Images are produced from the best available original document.

Contract No. W-7405-eng-26

ISOTOPIC POWER MATERIALS DEVELOPMENT
PROGRESS REPORT FOR MAY 1972

R. G. Donnelly

Metals and Ceramics Division

JUNE 1972

OAK RIDGE NATIONAL LABORATORY
Oak Ridge, Tennessee 37830
UNION CARBIDE CORPORATION
for the
U.S. ATOMIC ENERGY COMMISSION

page blank

CONTENTS

CLADDING MATERIALS PROGRAM

Characterization of Pt—Rh—W Alloys

J. H. Erwin and H. Inouye

We continued the evaluation of rolled Pt—Rh—W alloy sheet. Previously we reported[1] results of tensile and modified Olsen cup tests of two Pt—26% Rh—8% W sheets, Pt-1D with known tungsten segregation, and Pt-1ER without obvious tungsten segregation, following heat treatment in the range 900 to 1300°C. Bend test results of similarly heat-treated samples from the two sheets are summarized in Table 1. In this respect, these data verify the 1000 to 1100°C temperature range indicated by the tensile and cup tests as optimum heat treatment for the 21% cold-rolled alloy. The calculated elongation and bend strength are 25 to 50% higher than the values obtained from tensile tests. This is perhaps due to differences in sample geometry and calculation methods. Duplicate samples for a given heat treatment showed occasional wide differences in the bend angle to failure. Examination of the fractures reveal grain boundary separation in the less ductile samples. We associated the grain boundary fracture with tungsten segregation from previous experience with the Pt-1D sheet; however, examination of samples by metallography has not revealed any differences in grain boundaries of the samples.

The tensile properties of Pt—26% Rh—8% W (heat 1ER) specimens taken from an 0.030 × 12 × 12-in. sheet are shown in Table 2. These data show consistent and nondirectional properties for a given heat treatment. The ductility increases uniformly with temperature from approximately 11% at room temperature to approximately 50% at 1316°C. On the other hand, the reduction in area is seen to increase abruptly from approximately 6% at room temperature to 100% at and above 760°C. Table 3 shows that the calculated impact capabilities at 1316°C of the alloy [defined as 0.5(UTS + YS) × fracture strain] increases somewhat with the strain rate by virtue of corresponding increases in the ultimate tensile and yield strength. The impact values for T-111 and iridium are 11,000 and 7,400 in.-lb/in.[3], respectively. The superior impact values of the platinum alloy arise from the fact that the yield strength is about 86% of the ultimate strength and that the fracture ductilities are also higher than T-111 or iridium.

To determine the effect of the rhodium content in Pt—Rh—W alloys, we increased the rhodium content from the previous 26% to 30% at the 8% W level. One small ingot (heat Pt-4A) was fabricated into sheet in a manner similar to previous procedure with excellent results. An Olsen cup test on a blank heat treated for 1 hr at 990°C in vacuum produced a full 7/8-in.-diam hemisphere with only two small surface cracks. This is in contrast with failure of the Pt—26% Rh—8% W alloy (Pt-1ER) blank at a cup

---

[1]R. G. Donnelly, *Isotopic Power Materials Development Progress Report for April 1972*, ORNL-TM-3828, Oak Ridge National Laboratory.

Table 1. Bend Test Results of 0.030-in.-thick Platinum—Rhodium—Tungsten Alloy Sheet
(Standard 2T bend test at a rate of 0.2 in./min)

Heat Treatment (°C) (1 hr vac)	Maximum Bend Angle (deg)			Elongation (%)			Bend Strength (ksi)		
	Pt-1D[a]	Pt-1ER[b]	Pt-4A[c]	Pt-1D[a]	Pt-1ER[b]	Pt-4A[c]	Pt-1D[a]	Pt-1ER[b]	Pt-4A[c]
Transverse Samples Bent Parallel to Cold Rolling Direction									
900	61	53	55	12.3	11.6	11.7	309	332	329
950	86	55	x	17.2	12.0	x	286	304	x
990	x	99	108	x	19.0	>20	196	209	214
1000	65	x	x	13.4	x	x	258	x	x
1050	80	60	x	16.4	12.8	x	166	170	x
1100	81	50	108	16.5	10.7	>20	153	145	152
1200	37	x	x	8.2	x	x	131	x	x
1300	35	42	87	8.1	9.5	18.0	118	115	136
Longitudinal Samples Bent Transverse to the Cold Rolling Direction									
900	70	46	x	13.9	10.0	x	292	313	x
950	86	64	x	19.1	13.3	x	269	300	x
990	x	64	x	x	13.3	x	x	193	x
1000	88	x	x	17.2	x	x	234	x	x
1050	70	52	x	14.6	11.2	x	153	167	x
1100	89	50	x	17.4	10.6	x	141	143	x
1200	45	45	x	9.7	9.7	x	125	129	x
1300	40	46	x	8.7	9.8	x	112	118	x

[a] Pt—26% Rh—8% W sheet showing segregation of W.

[b] Pt—26% Rh—8% W sheet with no segregation indicated.

[c] Pt—30% Rh—8% W sheet.

x = no sample.

height of only 0.467 in. Results of the bend tests on this alloy are also given in Table 1. Samples heat treated at both 990 and 1100°C withstood a 90° 2T bend test.

Table 2. Tensile Properties of 0.030 × 12 × 12-in. Sheet
of Pt—26% Rh—8% W (Heat Pt-1ER)[a]

1-Hr Heat Treatment (°C)	Test Temperature (°C)	Ultimate Tensile Strength (psi)	Yield[b] Strength (psi)	Elongation (%)	Reduction in Area (%)
Longitudinal to Rolling Direction					
1000	Room	152,000	103,200	11.3	11.9
1100	Room	104,800	53,100	13.5	6.1
1200	Room	92,100	47,300	11.5	7.5
1300	Room	80,700	40,400	11.1	5.7
1200	760	74,400	28,700	27.8	∿100
1200	1093	38,400	18,900	30.8	∿100
1200	1316	17,000	14,900	52.0	∿100
Transverse to Rolling Direction					
1000	Room	150,300	109,700	13.8	15.3
1100	Room	101,000	55,000	13.3	5.3
1200	Room	91,600	49,400	11.3	7.2
1300	Room	74,800	42,000	9.3	6.0

[a]Cold rolled 21% before annealing (strain rate 0.05 in./in./min).

[b]0.2% offset yield strength.

Table 3. The Effect of Strain Rate on the Tensile Properties of
Pt—26% Rh—8% W Sheet at 1316°C[a]

Strain Rate (in./in./min)	Ultimate Tensile Strength (psi)	Yield[b] Strength (psi)	Elongation (%)	Impact Values[c] (in.-lb/in.^{3})
0.05	17,000	14,900	52.0	16,600
0.10	20,100	17,600	56.5	21,200
0.20	20,700	16,900	47.0	17,700

[a]0.030-in.-thick sheet of heat Pt-1ER annealed 1 hr at 1200°C.

[b]0.2% offset yield strength.

[c]0.5(UTS + YS) × fracture strain.

The tensile properties of heat Pt-4A are shown in Table 4. At room temperature this alloy is stronger and more ductile than Pt—26% Rh—8% W; however, at 1093 and 1316°C a significant amount of scatter was observed. Because the specimens showing poor tensile properties were taken from the same side of the rolled sheet, it is suspected that contamination or segregation has occurred.

Table 4. Tensile Properties of 0.030-in.-thick
Pt—26% Rh—8% W (Heat Pt-4A)[a]

Test Temperature (°C)	Ultimate Tensile Strength (psi)	0.2% Offset Yield Strength (psi)	Elongation (%)	Reduction in Area (%)
Longitudinal to Rolling Direction				
Room	115,000	53,200	17.8	9.1
1093[b]	38,000	20,500	16.8	13.4
1316	19,800	16,500	46.8	57
Transverse to Rolling Direction				
Room	108,200	50,800	18.8	9.1
760	75,100	30,200	30.2	35.1
1093[b]	35,700	19,500	18.3	35.4
1316[b]	15,500	15,000	28.0	11.9

[a]Specimens annealed 1 hr at 1200°C, tested at 0.05 in./in./min.

[b]Specimens showed numerous cracks in gage length after testing.

Characterization of Iridium

C. T. Liu

To show the effect of a heat pulse during re-entry of the MHW heat source on the tensile properties of iridium, sheet specimens were heated 5 min at 2000°C in vacuum after recrystallization for 1 hr at 1500°C. The tensile results for such a treatment are shown in Table 5 together with those reported previously.[2] The mechanical properties of the specimens recrystallized 1 hr at 1500°C alone (Case A in Table 5) behave normally in terms of temperature dependence of strength and ductility. The specimens subjected to the heat pulse (Case B in Table 5) behave abnormally as follows:

1. The yield strength is extremely low at low temperatures.

2. Both the ultimate and yield strengths show minimum values at 1093°C.

3. The ductility is low up to 1093°C, and it also has a minimum value (6.4%) at 1093°C.

4. The heat pulse has no effect on the ductility at the impact temperature, that is, 1316°C.

To characterize the fabricability of iridium, 1/8-in. iridium plate received from Engelhard Industries was warm-rolled at 825°C in air. This temperature was chosen because the oxidation rate of iridium is

---

[2]R. G. Donnelly, *Isotopic Power Materials Development Progress Report for December 1971*, ORNL-CF-72-1-13, Oak Ridge National Laboratory.

low below 900°C. The result indicates that the fabricability of iridium is good at 825°C. The rolled plate shows no surface or edge cracks when reduced to 55 mils with one intermediate anneal to 1280°C. A part of the stock was further rolled to 30 mils at room temperature. However, some surface cracks developed near the edge of the specimen.

Table 5. Tensile Properties of Iridium Specimens Under Two Heat Treatments:[a]

A — Recrystallized 1 hr at 1500°C
B — 5-min anneal at 2000°C after recrystallizing 1 hr at 1500°C

Testing Temp (°C)	Tensile Strength (psi)		Yield Strength (psi)		Elongation (%)	
	A	B	A	B	A	B
Room	56,000	46,100	25,000	11,500	5.7	8.5
1093	35,000	13,500	16,000	9,000[b]	39.6	6.4
1316	26,000	23,000	13,000	10,500	38	33.7

[a]0.020-in.-thick sheet, strain rate 0.05 in./in./min.

[b]The specimen shows discontinuous yielding.

Iridium Purification and Scrap Recycle

H. Inouye

A laboratory development effort directed toward the purification of iridium and leading to a process for producing high-purity iridium sheet has been initiated. Tentatively, two distinct routes are contemplated. First, commercial iridium powder as purchased from vendors will be treated in acids and hydrogen to remove impurities prior to melting. The second route constitutes the purification and/or recycling of scrap.

Some difficulty is being encountered in obtaining iridium from vendors. No iridium powder is on hand now for conducting the first part of the study. Consequently, the second route has become significantly more important to the overall program plan and is therefore being elevated to an active status.

Currently, a literature survey is being conducted on the dissolution and purification of iridium, and the available information should be evaluated this month. In the meantime, some preliminary experiments for the purification of iridium scrap by a pyrometallurgical process, which is described below, has been initiated.

Iridium is insoluble in most acids, and any dissolution method would also dissolve the impurities. Separation of iridium in this case would be from the soluble salts by a chemical process. The pyrometallurgical process takes advantage of the relatively high oxidation rate of iridium to gaseous

iridium oxide[3,4] in flowing oxygen and its separation from impurities as solid IrO_2. The condensed IrO_2 is then reduced to powder in H_2. To demonstrate feasibility, Ir—3 wt % Nb scrap was pulverized to a powder (as it is very brittle) to increase the surface area, then oxidized in flowing oxygen at 1100°C. Black crystals of IrO_2 deposited in the cooler portion of the quartz tube, and a solid white powder of Nb_2O_5 was left as a residue in the hot zone of the furnace tube. Based on the vapor pressures of the oxides at 1100°C, impurities, such as Si, Cr, Nb, Th, Fe, Al, Ni, Zr, Hf, etc., will be removed from impure iridium as solid oxide residues in the distillation retort. The condensate of IrO_2 which may contain oxides of Mo, W, or Re can be removed by acids or NH_4OH since IrO_2 is insoluble in these solvents. Carbon and sulfur impurities are oxidized to noncondensable gases under these conditions and are removed in this form.

REFRACTORY ALLOYS PROGRAM

Effect of Oxygen Contamination on the Mechanical Properties of Molybdenum-Base Alloys

C. T. Liu

Table 6 shows the effect of oxygen doping on the mechanical properties of TZM at the Pioneer impact temperature, that is, 1316°C. The ductility decreases seriously with doping time and is almost lost after 207 hr of exposure at 1000°C. Because tensile tests at lower temperatures showed the same behavior, one concludes that the ductility of oxygen-contaminated TZM does not improve with an increase in temperature.

Table 6. Tensile Properties at 1316°C of 20-mil-thick TZM Sheet Specimens Contaminated with Oxygen[a]

Doping Time (hr)	Elongation (%)	Tensile Strength (psi)
0	30	22,000
25	8.0	28,700
50	6.5	27,800
207	0.5	31,300

[a]Doped in 1×10^{-5} torr oxygen at 1000°C.

[3]J. R. Ogren *et al.*, *Radioisotope Propulsion Technology Program*, Vol. III, STL-517-0049 (Oct. 1966).

[4]C. B. Alcock and G. W. Hooper, *Proc. Royal Soc.* A254, 551-61 (1960).

Effect of Carbon Monoxide Contamination on the Mechanical Properties of Molybdenum-Base Alloys

C. T. Liu

TZM specimens were exposed to 1×10^{-5} torr CO at 1000°C for different periods of time to determine in simulation its compatibility with gases outgassed from graphite and Min-K 1301. The results of tensile tests are presented in Table 7. The tensile strength shows a general increase with doping time. The ductility at room temperature drops sharply between 240- and 500-hr exposures at 1000°C but remains constant at a value of approximately 30% at 1316°C. As shown in Table 7, the ductility after 1000 hr of exposure is a maximum at 825°C. TZM doped with CO behaves quite differently from that doped in oxygen. Complete characterization requires more data.

Table 7. Tensile Properties of 20-mil-thick TZM Sheet Specimens Contaminated with Cobalt at 1×10^{-5} Torr and 1000°C and Tested at Various Temperatures

Doping Time (hr)	Elongation (%)	Tensile Strength (psi)
	Room Temperature	
0	37	79,000
240	37.3	80,500
500	3.9	80,000
1000	1.1	83,800
	825°C	
0	24.8	45,000
1000	15.3	50,700
	1093°C	
0	24[a]	33,000[a]
1000	3.2	40,800
	1316°C	
0	30[a]	22,000
240	29	28,000
500	29.7	27,000

[a]Data collected from General Electric, *Multi-Hundred Watt, Radioisotope Thermoelectric Generator Program,* GESP-7034 (March 1970).

MATERIALS COMPATIBILITY TESTING FOR THE LASL-DART PROJECT

J. R. DiStefano

Compatibility couples involving several non-fuel materials being considered in constructing the DART were examined after 500 hr at 1300, 1400, and 1500°C, and the data are summarized in Tables 8-10. Only the couples tested at 1400°C were examined in detail.

From the data it would appear that graphite is very compatible with BeO, W, Re, and Pt—Rh—W up to 1500°C. In cases where W and Re cracked, it did not appear to be the result of interaction with the graphite and probably occurred during cutting and/or mounting.

All three oxides, ZrO_2, HfO_2, and BeO, showed good compatibility with the metals they were tested against. Visual observation indicated some discoloration of both ZrO_2 and HfO_2, and relatively large weight losses were noted in both those oxides. Beryllium oxide showed little tendency to interact even in the 1500°C tests that were examined. However, a rather serious mass transfer effect was found in the closed tungsten capsule that contained BeO. The tungsten showed rather large weight losses and had an etched appearance indicative of dissolution. Since this was not observed in the couple that was tested in dynamic vacuum, it seems likely that oxygen was involved in the process. One possible type of reaction is

$$W + x/2 = WO_x(g) \ .$$
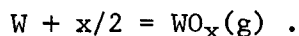
The source of oxygen is the BeO, and for vapor transport to occur, the reverse reaction must take place somewhere in the system. The driving force for the reverse reaction is difficult to postulate. An activity gradient could occur from a temperature gradient, pressure change, or energy change as a result of geometrical considerations. For a closed system of the type we have, it is hard to identify the reason for such an energy gradient to occur. However, we previously found the same type of thing when we exposed tungsten to Cm_2O_3.[5]

---

[5]J. R. DiStefano and K. H. Lin, *Compatibility of Curium Oxide with Refractory Metals at 1650°C and 1850°C*, ORNL-4773, Oak Ridge National Laboratory (March 1972), pp. 21-36.

Table 8. Summary of 1400°C Compatibility Test Data for LASL-DART Project

Sample No.	Couple	Visual Observation	Metallographic Observations	Chemical Analysis (wt %)		Hardness
				Carbon in Metal	Oxygen in Metal	
1B	C-Ta	R,S	Two layers on Ta surface to depth of 3 mils	0.024		Matrix = 112 DPH Layer = 1512 DPH
2B	C-W	NR	No interaction	0.0017		Matrix = 375 DPH
3B	C-Mo	R,D,S	Reaction zone in Mo to 27 mils deep	0.050		Matrix = 151 DPH Layer = 1100 DPH
4B	C-BeO	D	No interaction	0.020		
5B	C-Re	S	Re cracked. No surface reaction zone, but Re either heavily twinned or contains needle-like precipitates throughout	0.012		Matrix = 381 DPH
6B	C-(Mo-50% Re)	R,S,D	Reaction zone in Mo-50 wt % Re to 56 mils			Matrix = 343 DPH Layer = 1390 DPH
7B	C-(Pt-Rh-W)	R,S,D	Specimen joined to graphite, but no reaction zone. Surface of Pt-Rh-W slightly roughened.	0.02-1.03[a]		Matrix = 235 DPH
Mo-2	Mo-ZrO$_2$	F,C	No interaction		0.0059	
W-2	W-ZrO$_2$	F,C	No interaction		0.0008	
Ta-2	Ta-ZrO$_2$	F,C	No interaction		0.0280	
Mo-5	Mo-HfO$_2$	F,C,SR	No interaction		0.0130	
W-5	W-HfO$_2$	C	No interaction		0.0014	
Ta-5	Ta-HfO$_2$	F,C	Very slight (<0.1 mil) surface reaction		0.0300	

Table 8. continued

| Sample No. | Couple | Visual Observation | Metallographic Observations | Chemical Analysis (wt %) | | Hardness |
				Carbon in Metal	Oxygen in Metal	
Mo-8	Mo—BeO	NR	No interaction		0.0074	
Mo-11	Mo—BeO	NR	No interaction		0.0062	
W-8	W—BeO	NR	Slight surface roughness		0.0012	
W-11	W—BeO	NR,W has etched appearance	Slight surface roughness		0.0006	
Re-1	Re—BeO	NR	Re surface irregular structure either shows a Widmanstatten second phase precipitate or is very highly twinned		<0.0001	
(Mo-50 Re)-1	(Mo-50Re)- BeO	NR	Chain-like grain-boundary precipitate throughout Mo-50Re		0.0040	
Mo-14	Mo-Re	S	Three distinct layers in diffusion zone. Some voids in Mo-rich layer.			
W-14	W-Re	S	Samples parted when cut. Re surface rough; layer on W surface. Some voids in W.			
W-17	W-(Mo-50 Re)	NR	Chain-like grain boundary phase throughout Mo-50Re			
(Mo-50 Re)-3	(Mo-50Re)- Ir	D	Chain-like grain boundary phase throughout Mo-50Re			

[a]Some graphite stuck to surface of specimen. R = visible reaction; S = couple stuck together; SR = slight reaction; NR = no visible reaction; D = surface of specimen discolored; F = ceramic flaked, chipped, or cracked; C = ceramic discolored.

Table 9. Summary of 1500°C Compatibility Test Data for LASL–DART Project

Sample No.	Couple	Visual Observation	Metallographic Observations	Chemical Analysis (wt %)	
				Carbon in Metal	Oxygen in Metal
1C	C-Ta	S,R,D			
2C	C-W	S,R	W cracked – probably during cutting. Slight surface roughening.		
3C	C-Mo	S,R,D			
4C	C-BeO	R,D	No reaction	0.044	
5C	C-Re	S	Re badly cracked, but there was no evidence of reaction.	0.380	
6C	C-(Mo-50Re)	S,D			
7C	C-(Pt-Rh-W)	S,R,D	Reaction to depth of $\sim$1 mil	0.056	
Mo-3	Mo-ZrO_2	C,F,NR			
W-3	W-ZrO_2	C,F,NR			
Ta-3	Ta-ZrO_2	C,S			
Mo-6	Mo-HfO_2	C,F,SR			
W-6	W-HfO_2	C,NR			
Ta-6	Ta-HfO_2	C,SR			
Mo-9	Mo-BeO	NR	No reaction		
Mo-12	Mo-BeO	NR			
W-9	W-BeO	NR			
W-12	W-BeO	W has etched appearance	No reaction		
Re-2	Re-BeO	NR	Slight surface roughening. High degree of twinning or deformation lines in microstructure		
(Mo-50 Re)-2	(Mo-50 Re)-BeO	NR	Slight surface roughening.		
Mo-15	Mo-Re	S			
W-15	W-Re	S			
(Mo-50 Re)-4	(Mo-50 Re)-Ir	R			

R = visible reaction; S = couple stuck together; SR = slight reaction; NR = no visible reaction; D = surface of specimen discolored; F = ceramic flaked, chipped, or cracked; C = ceramic discolored.

11

Table 10. Summary of Weight Change Data on Compatibility Couples

Couple	Weight Change (mg)					
	1300°C		1400°C		1500°C	
	C	Metal	C	Metal	C	Metal
C-Ta	a	a	a	a	-4.1	+15.4
C-W	-0.7	0	-0.7	0	-2.2	+9.4
C-Mo	-7.7	+13.5	a	a	-1.2	-58.6
C-BeO	+0.6	-2.3	—	-3.6	-5.6	-75.7
C-Re	a	a	a	a	a	a
C(Mo-50Re)	a	a	-19	+38.7	a	a
C(Pt-Rh-W)	-1.2	+2.0	a	a	a	a
	Oxide	Metal	Oxide	Metal	Oxide	Metal
Mo-ZrO$_2$	b	b	-10.6	0	b	b
W-ZrO$_2$	b	b	-70.5	+3.0	b	b
Ta-ZrO$_2$	b	b	-41.8	+1.4	b	b
Mo-HfO$_2$	b	b	-116	+8.3	b	b
W-HfO$_2$	b	b	-11.9	+5.0	b	b
Ta-HfO$_2$	b	b	-60.0	+2.5	b	b
Mo-BeO	b	b	-5.5	0	-6.0	-0.2
Mo-BeO^c	b	b	-2.6	0	b	b
W-BeO	b	b	-4.6	+7.0	b	b
W-BeO^c	b	b	0	-2.5	-1.9	-610
Re-BeO	b	b	-4.1	+1.5	-4.0	0
(Mo-50Re)-BeO	b	b	-4.1	+1.0	-5.7	+4.2
	Metal 1	Metal 2	Metal 1	Metal 2	Metal 1	Metal 2
Mo^1-Re^2	b	b	0	d	b	b
W^1-Re^2	b	b	-1.5	d	b	b
W^1-(Mo-50Re)^2	b	b	0	+1.2	b	b
(Mo-50Re)^1-Ir^2	b	b	+4.8	-6.8	+3.4	-5.1

[a]Graphite stuck to metal.

[b]Sample not weighed.

[c]Closed capsule.

[d]Sample stuck to sample holder.

INTERNAL

1. G. M. Adamson, Jr.	16. H. C. McCurdy
2. P. S. Baker	17. R. E. McDonald
3. G. E. Boyd	18. R. E. McHenry
4. J. E. Cunningham	19. P. Patriarca
5. J. R. DiStefano	20. R. A. Robinson
6. R. G. Donnelly	21. A. F. Rupp
7. J. H. Erwin	22. A. C. Schaffhauser
8. J. H Frye, Jr.	23. D. B. Trauger
9. M. R. Hill	24. J. R. Weir
10. H. Inouye	25-26. Central Research Library
11. Lynda Kern	27. Document Reference Section
12. E. Lamb	28-29. Laboratory Records
13. C. T. Liu	30. Laboratory Records, ORNL-RC
14. E. L. Long, Jr.	31. ORNL Patent Office
15. W. R. Martin	

EXTERNAL

32. R. Andelin, Donald W. Douglas Laboratories
33-34. R. D. Baker, Los Alamos Scientific Laboratory
35. V. Berniklau, Albuquerque Area Office, AEC
36. W. Brooksbank, G. C. Marshall Space Flight Center, NASA
37. R. Brouns, Langley Research Center, NASA
38. R. T. Carpenter, Division of Space Nuclear Systems, AEC
39. W. T. Cave, Monsanto Research Corporation
40. G. R. Crane, Andrews AFB
41. D. D. Davis, Dayton Area Office, AEC
42. G. Deutsch, NASA Headquarters
43. G. P. Dix, Division of Space Nuclear Systems, AEC
44. J. Epstein, Goddard Space Flight Center, NASA
45. R. Fischell, Johns Hopkins University
46. N. Goldenberg, Division of Space Nuclear Systems, AEC
47. R. J. Hart, AEC-ORO
48. A. Hoffman, TRW Systems
49. W. S. Hollman, Division of Applied Technology, AEC
50. R. G. Ivanoff, Jet Propulsion Laboratory
51. H. Jaffe, Division of Space Nuclear Systems, AEC
52. T. B. Kerr, NASA Headquarters
53. M. Klein, Division of Space Nuclear Systems, AEC
54. G. Linkous, Isotopes, Inc.
55. J. J. Lombardo, Lewis Research Center, NASA
56. M. MacWilliams, Kirtland AFB
57. J. McDonald, Sandia Laboratories
58. H. Nelson, Ames Research Center, NASA
59. G. A. Newby, Division of Space Nuclear Systems, AEC
60. A. Noonan, Kirtland AFB
61. W. Pardue, Battelle Memorial Institute
62. A. A. Pitrolo, General Electric Company
63. T. W. Redding, Manned Spacecraft Center
64. F. Schulman, AEC Headquarters

65. M. Shaw, Division of Reactor Development and Technology, AEC
66. R. W. Shivers, Division of Applied Technology, AEC
67. J. M. Simmons, Division of Reactor Development and Technology, AEC
68. H. C. Slone, Lewis Research Center
69. M. D. Starr, Naval Facilities Engineering Command
70. R. Valle, Monsanto Research Corporation
71. E. J. Wahlquist, Division of Space Nuclear Systems, AEC
72. A. Wilbur, Ames Research Center, NASA
73. Research and Technical Support Div., ORO
74-75. Technical Information Center, OR